ELSEVIER

Biophysical Chemistry 125 (2007) 213–220

Biophysical Chemistry

http://www.elsevier.com/locate/biophyschem

A micelle nucleation model for the interaction of dodecyl sulphate with Lys49–phospholipases A_2

Raquel Kely Bortoleto-Bugs [a], Milton Roque Bugs [a], Augusto Agostinho Neto [a], R.J. Ward [b,*]

[a] *Department of Physics, IBILCE/UNESP, São José do Rio Preto-SP, Brazil*

[b] *Department of Chemistry, Faculdade de Filosofia Ciências e Letras de Ribeirão Preto, Universidade de São Paulo, Avenida Bandeirantes 3900, Monte Alegre, CEP 14049-901, Ribeirão Preto-SP, Brazil*

Received 10 May 2006; received in revised form 3 August 2006; accepted 4 August 2006
Available online 11 August 2006

Abstract

Bothropstoxin-I (BthTx-I) is a Lys49–PLA_2 from the venom of *Bothrops jararacussu* that lacks detectable catalytic activity, yet causes rapid Ca^{2+}-independent membrane damage. With the aim of understanding the interaction between BthTx-I and amphiphilic molecules, we have studied the interaction of sodium dodecyl sulphate (SDS) with the protein. Circular dichroism and attenuated total reflection Fourier-transform infrared spectra of BthTx-I reveal changes in the α-helical organization of the protein at an SDS/BthTx-I molar ratio of 20–25. At SDS/BthTx-I ratios of 40–45 the α-helices return to a native-like conformation, although fluorescence emission anisotropy measurements of 2-amino-*N*-hexadecyl-benzamide (AHBA) demonstrate that the total SDS is below the critical micelle concentration when this transition occurs. These results may be interpreted as the result of SDS accumulation by the BthTx-I homodimer and the formation of a pre-micelle SDS/BthTx-I complex, which may subsequently be released from the protein surface as a free micelle. Similar changes in the α-helical organization of BthTx-I were observed in the presence of dipalmitoylphosphatidylcholine liposomes, suggesting that protein structure transitions coupled to organization changes of bound amphiphiles may play a role in the Ca^{2+}-independent membrane damage by Lys49–PLA_2s.

Keywords: Bothropstoxin-I; Circular dichroism; Fluorescence anisotropy; ATR-FTIR

1. Introduction

Phospholipases A_2 (PLA_2 – EC 3.1.1.4) catalyze the hydrolysis the *sn*-2 acyl bonds of *sn*-3 phospholipids [1], and are currently classified into 14 groups based on disulphide bonding patterns and amino acid sequence similarity [2]. The association of $sPLA_2$ with phospholipid membranes results in a significant increase in the hydrolytic activity, and the interaction between class I/II phospholipase A_2 with the target membrane has been extensively studied [3,4], and this work has led to the development of the so-called "enzyme" and "substrate" models of interfacial activation. The "enzyme" models suggest that the lipid substrate induces structural changes in the protein which optimize the active site conformation and catalytic efficiency [5–7], whereas "substrate" models emphasize the modulation of catalytic activity by the physico-chemical membrane characteristics such as fluidity, curvature and the surface charge of aggregated membrane phospholipids [8,9]. However, the differences between "enzyme" and "substrate" models might not be so clear-cut, and it has been suggested that the "enzyme" and "substrate" models are not mutually exclusive [3]. Indeed, it has been demonstrated that the interaction between $sPLA_2$ and phospholipid membranes results in synergistic changes of both structures [10], which implies coupling between the protein and amphiphilic molecules in the membrane.

With the aim of further understanding the protein/membrane coupling of $sPLA_2$ we have studied the effects of the interaction between amphiphilic molecules and the bothropstoxin I (BthTx-

Abbreviations: PLA_2, phospholipase A_2; Lys49–PLA_2, a family of PLA_2 homologues with Lys at position 49; BthTx-I, Lys49–PLA_2 homologue isolated from the venom of *Bothrops jararacussu*; SDS, sodium dodecyl sulphate; DPPC, dipalmitoylphosphatidylcholine; CD, circular dichroism spectroscopy; ATR-FTIR, attenuated total reflection Fourier-transform infrared spectroscopy; AHBA, 2-amino-*N*-hexadecyl-benzamide; CMC, critical micelle concentration; CMC_{SDS}, CMC of pure SDS; CMC_P, measured CMC of SDS in the presence of BthTx-I.

* Corresponding author. Tel.: +55 16 3602 4384; fax: +55 16 3602 4838.
E-mail address: rjward@fmrp.usp.br (R.J. Ward).

0301-4622/$ - see front matter © 2006 Elsevier B.V. All rights reserved.
doi:10.1016/j.bpc.2006.08.002

I), a homodimeric class IIA Lys49–PLA_2 isolated from the venom of *Bothrops jararacussu* [11], in which the aspartic acid at position 49 (Asp49) in the catalytic site is substituted by a lysine (Lys49) [12]. Although lacking detectable hydrolytic activity [13], the BthTx-I shows cytolytic effects [14] and in common with other Lys49–PLA_2s retains a Ca^{2+}-independent membrane damaging activity, as demonstrated by the rapid release of the aqueous content of liposomes on interaction with the protein [15–18]. We have recently described the activation of this membrane damaging activity by the binding of ~4 SDS molecules to specific sites on the BthTx-I homodimer [19]. Although activation is essential for Ca^{2+}-independent membrane damaging activity, the permeabilization of phospholipid bilayer clearly requires the perturbation of significantly greater numbers of amphiphiles, which has led us to investigate the interaction of SDS with BthTx-I at higher surfactant/protein ratios.

Here we present the results of the titration of BthTx-I both with the surfactant sodium dodecyl sulphate (SDS) and with the phospholipid dipalmitoylphosphatidylcholine (DPPC) in aqueous solution. Using circular dichroism (CD) and attenuated total reflection Fourier-transform infrared spectroscopy (ATR-FTIR), we describe changes in protein structure that are correlated with changes in the fluorescence emission anisotropy of the amphiphilic 2-amino-*N*-hexadecyl-benzamide (AHBA) bound to the BthTx-I. A model is presented in which accumulation of amphiphilic molecules by BthTx-I drives a process in which protein structural changes are coupled to transitions in the aggregation state of the associated amphiphiles.

2. Materials and methods

2.1. Protein purification and sample preparation

Bothropstoxin-I (BthTx-I) was purified from whole *B. jararacussu* venom using a combination of cation-exchange and size exclusion chromatography as previously described [20]. Protein purity was routinely evaluated by silver staining of SDS–PAGE gels, and aliquots of purified protein were stored at 4 °C and used within 10 days. For spectroscopic analyses the BthTx-I samples were prepared in 25 mM Tris–HCl pH 7.0, with a NaCl concentration of between 50 and 150 mM at final protein concentrations of 35–150 μM. The chemicals used in this study were obtained from reputable manufacturers, and were all of analytic grade.

2.2. Attenuated total reflection Fourier-transform infrared spectroscopy (ATR-FTIR)

The ATR-FTIR spectra of BthTx-I and SDS/BthTx-I mixtures were recorded in the horizontal ATR mode using a Nicolet Nexus 670 FTIR spectrometer (Nicolet Instrument Co, Madison, WI, USA) equipped with a DTGS-KBr detector with a ZnSe crystal at a nominal incident angle of 45°. The spectrometer was continuously purged with nitrogen gas to eliminate water vapour and CO_2 from the sample compartment. The protein sample at a concentration of 150 μM was placed in an ATR cell and spectra were measured at 25 °C after successive additions of fixed aliquots of SDS. The signal-to-noise ratio was improved by increasing the number of scans, and the final spectra were the average of 512 scans of the non-smoothed protein vibrational spectra recorded at a resolution of 2 cm^{-1} over the wave number range of 4000–400 cm^{-1}. Under these conditions the Amide I mode is overlapped by many defined features arising from the rotation–vibration spectrum of water, therefore the signals from the aqueous buffer were recorded under identical conditions as the sample spectra and digitally subtracted to obtain a straight baseline between 2000 and 1800 cm^{-1}. All measurements were repeated three times confirming that the observed intensity changes are the result of the interaction of SDS with protein rather than the consequence of altered humidity conditions inside the instrument.

2.3. Circular dichroism (CD) spectroscopy

The far ultraviolet circular dichroism (far-UVCD) spectra of BthTx-I were measured with a Jasco 810 spectropolarimeter using either 0.01 cm or 0.2 cm path length quartz cuvettes with a 10 nm bandwidth, with the temperature maintained at 298 K. The measurements were made between 190 and 250 nm with a 0.5 nm resolution taking the average of 5 accumulated scans. All protein spectra were corrected by subtraction of the spectra of buffer alone. For titration experiments in which the concentration of SDS was altered, the initial protein concentration was between 37 and 97 μg mL^{-1}, to which were added aliquots of stock SDS solutions to final concentrations of between 200 μM and 40 mM. Titrations were also made using liposomes composed of the zwitterionic phospholipid dipalmitoylphosphatidylcholine (DPPC, Sigma-Aldrich) in the presence of SDS at an initial protein/SDS molar ratio of 1:4. Liposomes were prepared by reverse phase evaporation [21] in aqueous buffered solution (150 mM NaCl, 25 mM Tris pH 7.0). The liposomes were passed through a 400 nm polycarbonate filter prior to use. In all titration experiments, the CD spectra over the range of 200–250 nm were measured in as described above.

2.4. HexAbz fluorescence anisotropy

BthTx-I at a concentration of 37 μM was incubated with a mixture of 37 μM AHBA [22] and 190 μM SDS to give a protein/total amphiphile molar ratio of 1:6, and this mixture was titrated with SDS over the concentrations range of 250 μM to 40 mM. The HexAbz fluorescence anisotropy was measured using an SLM fluorimeter equipped with Glan-Thompson quartz polarizers at a fixed emission wavelength of 480 nm with the excitation wavelength set to 320 nm. Excitation and emission band pass were fixed at 4 nm, and the emission signals from a buffer blank were subtracted from the experimental data prior to the anisotropy calculation.

3. Results

In the absence of SDS (Fig. 1A), the far-UVCD spectrum of the BthTx-I shows minima at 208 and 222 nm, which is

characteristic of a protein rich in α-helix and is consistent with the high α-helical content of BthTx-I observed in the crystal structure [23]. As shown in Fig. 1B, at an SDS/protein ratio of 24 the minimum at 208 nm is significantly reduced, and the minimum at 222 nm is shifted to 230 nm. As shown in Fig. 1C, at an SDS/BthTx-I ratio of 119 the far-UVCD spectrum reverts to a profile and intensity similar to that of the protein alone. The changes in the profile of the far-UVCD spectrum at the SDS/BthTx-I ratio of 25 is accompanied by an increase in the turbidity of the solution and Fig. 1A–C show that at two optical path lengths of 0.2 mm and 0.01 mm, similar changes in the CD spectra profiles were observed. This suggests that the changes in the CD spectra are due to structural changes in the protein rather than light scatter artifacts, which is in accord with previous observations demonstrating that light scatter does not influence the profile of CD spectra of $sPLA_2$ in the far-UV region [24].

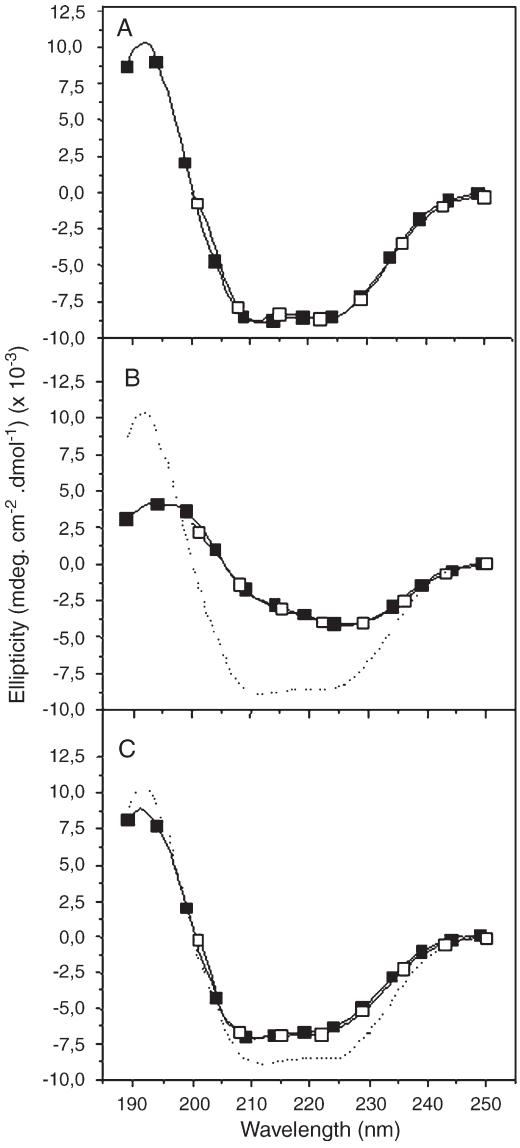

Fig. 1. The effect of SDS on the far-UVCD spectrum of BthTx-I. The BthTx-I far-UV circular dichroism spectra measured with 0.2 cm (open squares) and 0.01 cm (closed squares) path length cuvettes on titration with (A) 0 μM, (B) 900 μM and (C) 4400 μM SDS to give SDS/BthTx-I molar ratios of 0, 24 and 119, respectively. The dotted lines in panels B and C show the far-UVCD spectrum for BthTx-I in the absence of SDS for comparison. The protein concentration was 37 μM and all measurements were made in 25 mM Tris–HCl pH 7.0, 150 mM NaCl.

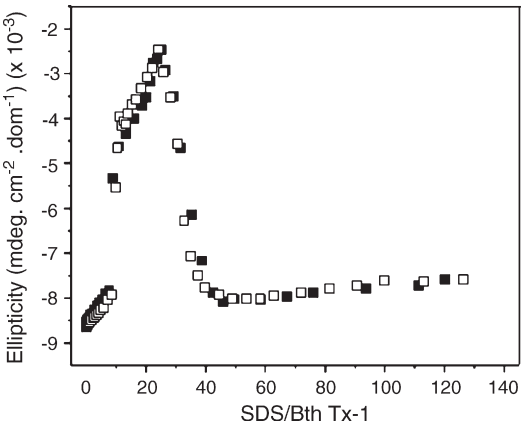

Fig. 2. The effect of protein concentration on the far-UVCD signal of BthTx-I on titration with SDS. Representative results showing changes in the molar ellipticity at 222 nm with increasing SDS/BthTx-I molar ratios. Ellipticity values were measured during a titration with SDS over the concentration range of 0 to 9 mM at BthTx-I concentrations of 47 μM (closed squares) and 93 μM (open squares).

The main panel in Fig. 2 shows the ellipticity changes at 222 nm as a function of the SDS/BthTx-I molar ratio at protein concentrations of 43 and 97 μM. After a gradual ellipticity increase over the SDS/BthTx-I ratios of 0 to 10, a maximum value is observed at ~25 SDS molecules per BthTx-I monomer, and at SDS/protein ratios of between 40 and 50 the ellipticity decreases to values of around −8000 mdeg cm^{-2} dmol^{-1}. Further addition of SDS causes only a slight increase in the ellipticity value. These results show that as the concentration of protein increases the SDS/BthTx-I molar ratios at which the ellipticity changes occur are constant, and suggests that SDS/protein ratios below ~50, effectively all the SDS is associated with the BthTx-I molecule. The profile of the far-UVCD spectrum is highly sensitive to subtle deviations from the canonical α-helical backbone dihedral angles [25,26]. The changes in the far-UVCD spectrum of the BthTx-I at SDS/protein ratios of ~25 have been interpreted as arising from subtle distortion of the α-helices of the protein [19], in which the reorientation of the amide plane of the peptidyl groups relative to the α-helix axes results in a reduction in the intensity of the amide π–π* transition exciton centered at 208 nm [27,28]. The return to a native-like far-UVCD profile at higher SDS/protein ratios suggests that under these conditions the distortion in the α-helices is reversed.

With the aim of further understanding these secondary structure changes of the BthTx-I, ATR-FTIR spectra of BthTx-I between wave numbers of 1700 and 1600 cm^{-1} (amide I region) were measured in the absence of SDS and at increasing SDS/BthTx-I ratios (Fig. 3A). At SDS/BthTx-I ratios of 18, the absorption is approximately 5-fold that of the native BthTx-I (Fig. 3B) and demonstrates a predominant band at 1652 cm^{-1}. This band arises from α-helices [29], and suggests that these structures become more stretched. This conclusion is supported

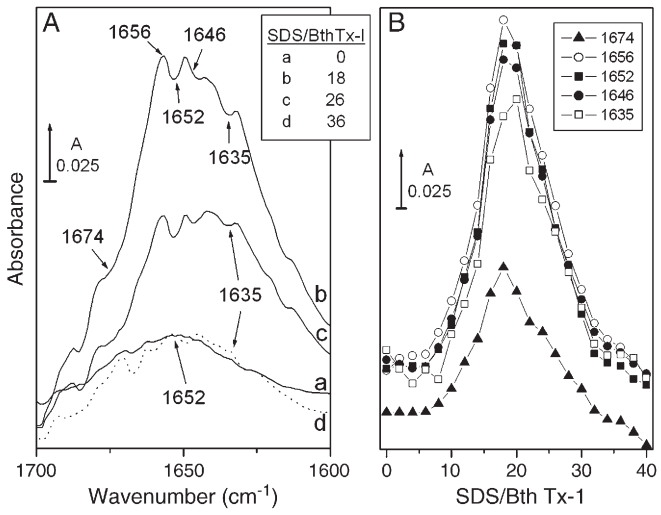

Fig. 3. The effect of SDS on the ATR-FTIR spectra of BthTx-I. (A) The main panel shows representative absorbance spectra measured in the wavenumber range of 1700–1600 cm^{-1} for the SDS/BthTx-I ratios of 0 (a), 18 (b), 26 (c) and 36 (d). The experiments were performed at a protein concentration of 150 μM as described in materials and methods. (B) Effect of SDS on the BthTx-I monitored at wave numbers of 1674, 1656, 1652, 1646 and 1635 cm^{-1}. The increased concentration of SDS is presented as a function of the molar ratio of SDS/BthTx-I.

by the overall increase in the intensity between 1700 and 1600 cm^{-1} that is indicative of peptide group (C=O) stretching on interaction of SDS with the protein. These observations are in agreement with the interpretation that association of surfactant with the BthTx-I results in the perturbation of the conformation of α-helices. On further addition of SDS, the intensity of the spectrum decreases, and at an SDS/BthTx-I ratio of between 35 and 40 returns to the initial absorption level demonstrating that the alteration in the α-helical conformation is reversible. Since ATR-FTIR uses micrometer range wavelengths, artifacts associated with light scattering are generally considered to be insignificant, and these results provide supportive evidence for reversible structural changes of the SDS/BthTx-I complex.

Further insights as to the formation and properties of the SDS/BthTx-I complex were gained by evaluating the effect of the addition of SDS on the far-UVCD signal of the BthTx-I at 222 nm at NaCl concentration between 50 and 150 mM. Fig. 4 shows that at all ionic strengths tested the spectral profile changes on titration with SDS are similar, and that the ellipticity at 222 nm increases at SDS/BthTx-I ratios of ~10 to reach maximum values at SDS/BthTx-I ratios of 20–25. The arrows in Fig. 4 indicate the critical micelle concentration (CMC) of

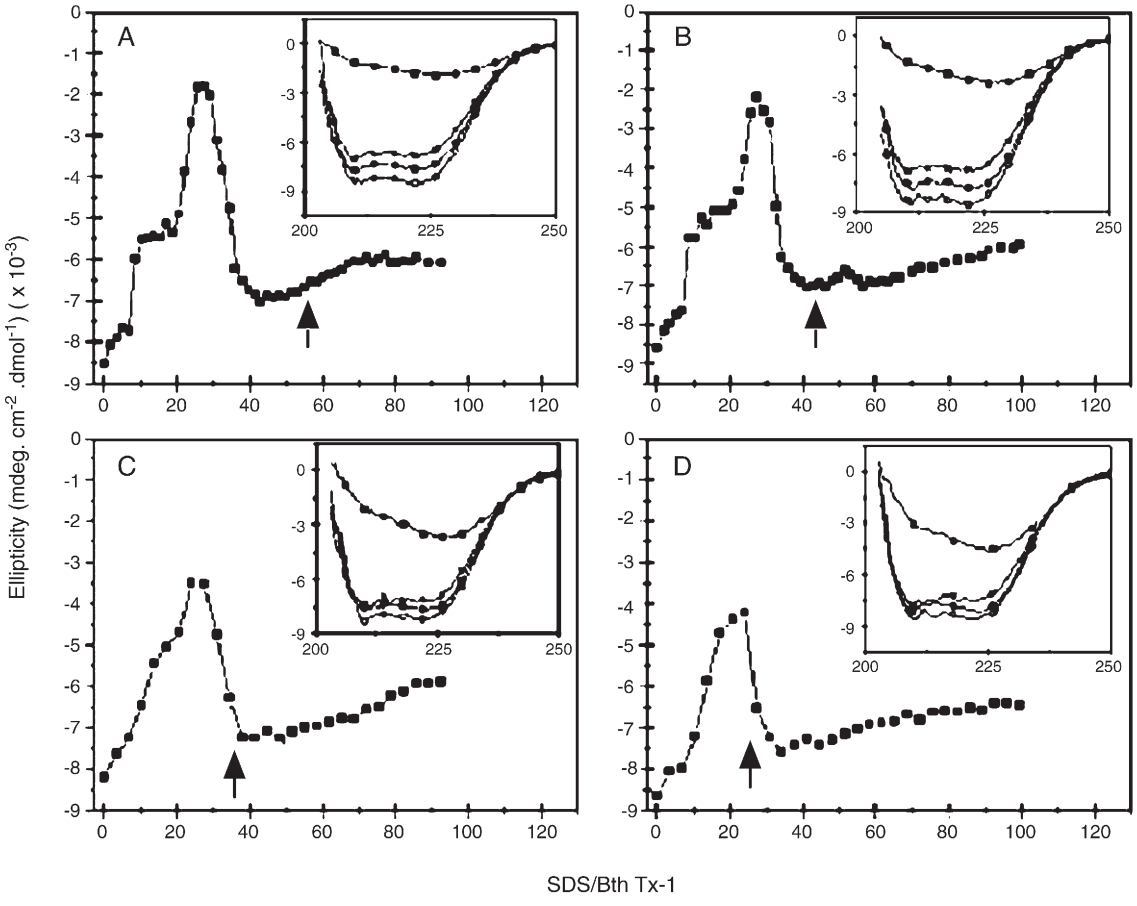

Fig. 4. Effect of SDS on the BthTx-I far-UVCD signal at 222 nm at various ionic strengths. The main panels present the molar ellipticity values of BthTx-I at 222 nm were measured on titration with SDS in the presence of (A) 50 mM, (B) 75 mM, (C) 100 mM and (D) 150 mM NaCl. The arrows indicate the critical micelle concentrations of the SDS at the given ionic strength. The protein concentration in these experiments was 35 μM. The inserts for each titration show the CD spectra measured in with 0.2 cm path length quartz cuvettes at SDS/BthTx-I ratios of 0 (open circles), 5 (closed circles), 25 (closed squares) and 40 (crosses).

pure SDS in solution, which as previously observed, increases with decreasing ionic strength [30]. These results demonstrate that the secondary structure changes observed in the BthTx-I are not correlated with the CMC of the SDS. Therefore the α-helical transitions observed in the SDS/BthTx-I complex are not due to the interaction of the protein with pre-formed SDS micelles, but is a consequence of the accumulation of SDS on the surface of the protein. Furthermore, these data suggest that the accumulation of defined numbers of surfactant molecules on the BthTx-I results in the reversible distortion of the α-helices in the protein.

With the aim of monitoring the binding of surfactant molecules to the BthTx-I, a series of titrations were performed in the presence of the fluorescent amphiphile HexAbz. In the presence of SDS below the CMC, the HexAbz has a fluorescence emission anisotropy value of ~0.015, which indicates a rapid motion of the uncomplexed molecule free in solution. As shown in Fig. 5, the HexAbz anisotropy increases to values of between 0.12 and 0.15 in the presence of BthTx-I, demonstrating that the fluorophore becomes immobilized on binding to the surface of the protein. Fig. 5A to 5D present the changes in HexAbz fluorescence anisotropy at increasing SDS/BthTx-I ratios at NaCl concentrations between 50 and 150 mM NaCl. The insets to Fig. 5A–D present the anisotropy changes as a function of total SDS concentration over the same NaCl concentration range. After an initial spike in the HexAbz

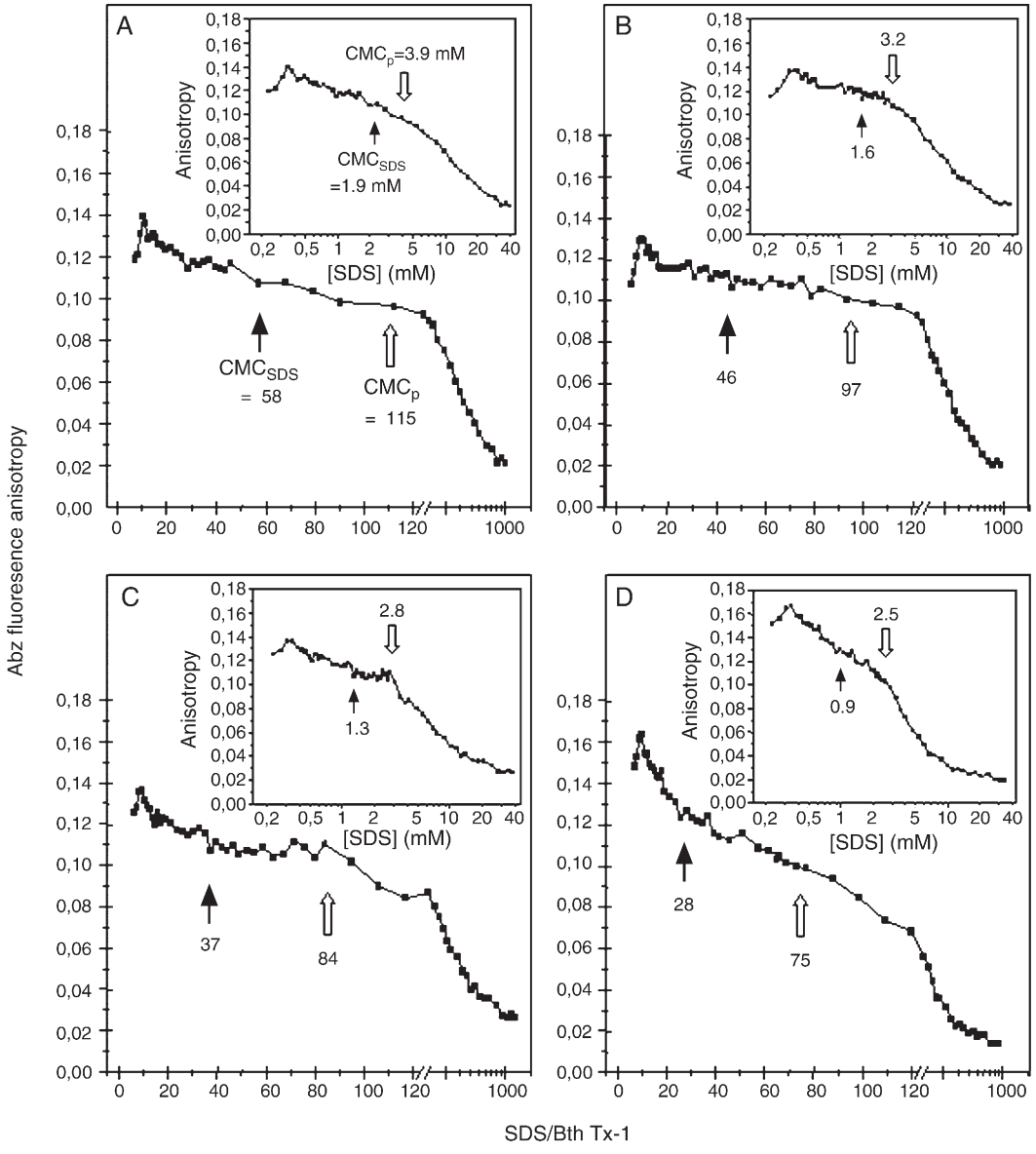

Fig. 5. The effect of SDS on the HexAbz fluorescence emission anisotropy. The main panels shown the changes in anisotropy as a function of SDS/BthTx-I molar ratio at concentrations of (A) 50, (B) 75, (C) 100 and (D) 150 mM NaCl. The inset to each figure presents the anisotropy change as a function of total SDS concentration. The critical micelle concentrations of pure SDS (CMC_{SDS}) is indicated by the solid arrow together with the value of the CMC. The open arrow shows the estimated critical micelle concentrations of the SDS in the presence of BthTx-I (CMC_P). The open and closed arrows in the main panels identify the SDS/BthTx-I molar ratios at which these two CMC values occur, together with their estimated values. All measurements were made at a protein concentration of 37 μM, in the presence of 25 mM Tris–HCl at pH 7.0. The experimental anisotropy measurement error was ±0.003.

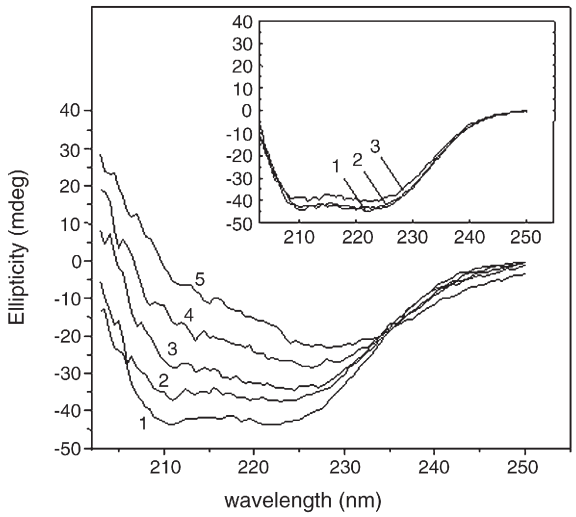

Fig. 6. The effect of addition of DPPC liposomes in the presence of SDS at a 1:4 surfactant/protein ratio (main panel) and in the addition of DPPC liposomes to BthTx-I in the absence of SDS (inset). The final concentrations for the titration shown in the main panel were; BthTx-I alone (curve 1), BthTx-I+83 μM SDS (curve 2), BthTx-I+83 μM SDS+14 μM DPPC (curve 3), BthTx-I+83 μM SDS+266 μM DPPC (curve 4) and the repeat of measurement in curve 4 after 1 h of incubation (curve 5). The final concentrations for the titration shown in the inset were BthTx-I alone (curve 1), BthTx-I+238 μM DPPC (curve 2) and the repeat of measurement in curve 2 after 1 h of incubation (curve 3) (B). All experiments were made at a protein concentration of 19 μM in the presence of 25 mM Tris–HCl pH 7.0, 150 mM NaCl.

anisotropy between 200 and 500 μM SDS, the anisotropy signal gradually decreases with increasing SDS concentration until a transition point is reached, above which the anisotropy signal decreases to a final value of ~0.025. Since titration of SDS in the absence of BthTx-I yielded HexAbz fluorescence anisotropy values of ~0.025 at SDS concentrations above the CMC (data not shown), we interpret this anisotropy transition as the consequence of SDS micelle formation. The inserts to Fig. 5 indicate the critical micelle concentrations for pure SDS in solution (CMC_{SDS}), together with the SDS concentration at which the HexAbz anisotropy transition is observed in the presence of protein (CMC_P). In all experiments the value of the CMC_{SDS} is less than the CMC_P, and the main panels in Fig. 5 show that at all ionic strengths the difference between the two CMC values is 1.4 to 1.6 mM, which corresponds to 35–40 molecules of SDS per BthTx-I, which is the number of SDS molecules per BthTx-I monomer that are removed from the solution due to association with the protein.

It has previously been demonstrated that binding of 4 molecules of SDS to the BthTx-I activates the calcium-independent membrane-damaging activity against liposome membranes [19]. In order to evaluate whether the α-helical changes observed in the SDS/BthTx-I complex are representative of changes in the phospholipid/BthTx-I complex on association with liposome membranes, BthTx-I was activated by pre-incubation with SDS at a surfactant/protein molar ratio of 4, and this mixture was subsequently titrated with DPPC liposomes. Fig. 6 shows that the profile changes of the far-UVCD spectra of the BthTx-I on titration with DPPC are similar to those observed on titration with SDS (compare Fig. 6 with Figs. 1 and 4). The insert to Fig. 6 shows that titration of BthTx-I with DPPC liposomes in the absence of SDS (conditions where the membrane damaging activity of BthTx-I is not activated) did not result in significant changes in the far-UVCD spectra. This result suggests that the structural changes on formation of the complex between phospholipids and the activated form of the BthTx-I are similar to those observed on the formation of the BthTx-I/SDS complex, and is in accord with the alteration of the internal α-helical organization that has previously been proposed for $sPLA_2$ bound to phospholipid bilayers [31].

4. Discussion

Binding of 4 molecules of SDS to BthTx-I is associated with the activation of the Ca^{2+}-independent membrane damaging activity of the protein, and also triggers the protein mediated conversion of phospholipid liposome membranes into structures resembling micelles [19]. In the present study, we have extended our investigation to include the effects of SDS binding at higher SDS/BthTx-I ratios. The collection of 35–40 surfactant molecules by the BthTx-I is spontaneous and we suggest that the binding surface is comprised of a hydrophobic phospholipid binding cleft surrounded by a ring of polar residues which defines the membrane interface recognition site (IRS) [32] or "i-face" [33], and which is a conserved structural feature of all class I/II PLA_2s. As shown in Fig. 7, lysine and arginine residues surround the IRS hydrophobic surface of the BthTx-I, which gives a pronounced cationic character to the region. Of the 24 positively charged amino acid residues in each monomer, 12 contribute to form a ring of cationic residues around the IRS of the BthTx-I, and Fig. 7 also shows that in the homodimeric form of the BthTx-I the dimer interface and IRS surfaces of each monomer merge to form an extended hydrophobic surface within a ring of cationic residues. The positions of the cationic residues at the IRS and dimer interface regions of the BthTx-I suggest that the bound SDS will be oriented with the anionic sulphate group of the SDS interacting with the cationic side chains of the protein, with the aliphatic region of the SDS making contact with non-polar amino acid side chains. These interactions would result in "bridging"

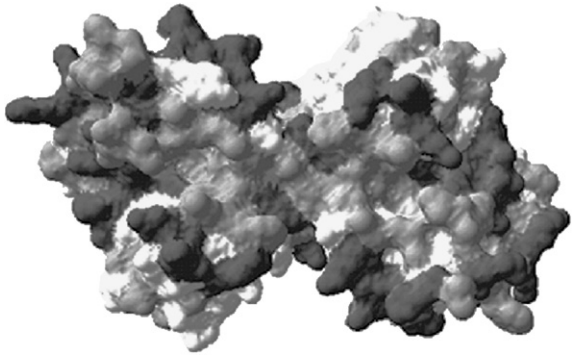

Fig. 7. (A) Solid surface representation of the BthTx-I homodimer viewing the interface recognition surface (IRS) which makes contact with the membrane. The homodimer presents an extended surface of exposed hydrophobic residues (shown in light grey) surrounded by a ring of positively charged residues (shown in dark grey) that forms an extended hydrophobic/cationic surface.

between charged residues at the rim and hydrophobic residues in the centre of the IRS surface. Further analysis of the crystal structure of the BthTx-I reveals that 8 of the 24 cationic residues in the BthTx-I are located on one of the three major α-helices of the protein. It is therefore reasonable to predict that binding of SDS would result in strain and distortion of these secondary structure elements.

Perhaps more surprising are the results demonstrating that on accumulation of 40–45 SDS molecules per monomer, the distortion of the α-helices is eliminated and they return to a native-like conformation. At this SDS/protein ratio, approximately 80–90 molecules of SDS are bound per BthTx-I dimer, and this total number of bound SDS molecules is similar to the mean aggregation numbers of SDS at the concentrations of NaCl used in our experiments [34]. It therefore becomes feasible that the bound surfactant reorganizes to form a micelle-like structure that remains associated as a "pre-micelle" complex with the protein. Under these conditions, the SDS molecules may exchange between environments dominated either by SDS/protein or by SDS/SDS interactions, reducing the overall strain on the protein α-helices. This increased overall mobility of the bound surfactant would also explain the gradual reduction in the fluorescence emission anisotropy of the bound HexAbz. It should be noted that previous studies have suggested that the formation and dynamics of the SDS/protein complex are not straightforward [35–37]. However, the formation of the SDS/BthTx-I complexes is a reversible process, and above the value of the CMC in the presence of protein (CMC_{prot}), these complexes dissociate, which opens the possibility that SDS molecules may be exchanged between protein molecules.

Evidence in favour of SDS exchange is provided by the HexAbz anisotropy changes that are observed around the CMC_{prot} (see Fig. 5). The rapid anisotropy decrease above this concentration shows that HexAbz has been transferred from the protein to micelles, which supports the suggestion that the SDS "pre-micelles" may dissociate from the surface of the BthTx-I. At free surfactant concentrations less than the CMC_{prot} the released SDS would rapidly form surfactant monomers, and the IRS surface of the BthTx-I dimer would again accumulate this surfactant from the solution. However, at total SDS concentrations above the CMC_{prot}, the released SDS would remain in the form of a micelle. This cycle of SDS capture, pre-micelle formation and release by the BthTx-I IRS would therefore explain the observed transfer of the HexAbz from the protein to micelles at high SDS concentrations.

A key feature in the micelle nucleation is the accumulation of SDS at the IRS of the BthTx-I dimer, and it is noteworthy that the accumulation of amphiphilic molecules by $sPLA_2$ has previously been observed in the monomeric PLA_2 from the venom of *Naja melanoleuca* [38] and in the Human Group X $sPLA_2$ [39]. More recently, a detailed model has been developed to describe the interaction between SDS and the porcine pancreatic group IB PLA_2 in which stepwise binding of approximately 35 molecules SDS by the protein results in the aggregation of the PLA_2/SDS complex [36,37]. The porcine PLA_2 is monomeric, and the IRS will therefore have a limited SDS binding capacity as compared to the extended dimeric IRS of the BthTx-I that can accumulate sufficient SDS to stabilize a pre-micelle complex.

Understanding the interaction of SDS with the BthTx-I may provide insights as to the Ca^{2+}-independent membrane damaging activity of the Lys49–PLA_2s. It has been previously proposed [23,40] that binding of the BthTx-I dimer to the membrane triggers a change in the protein conformation, and here we have demonstrated that the structural changes in the activated BthTx-I induced by DPPC liposomes are similar to those induced by SDS. The alteration in the α-helical organization that is observed on the interaction of activated BthTx-I with DPPC liposomes leads us to suggest that a micelle nucleation mechanism involving membrane lipids is coupled to protein structure transformations, that may result in the reorganization of bilayer phospholipids molecules and thereby result in the Ca^{2+}-independent membrane damaging activity of BthTx-I. We speculate that on binding of the BthTx-I dimer to the membrane, the phospholipids are at first perturbed and then collected at the IRS of the protein. This event is coupled with changes in the BthTx-I structure and the reorganization of the phospholipids in the membrane bilayer, and leads to the loss of the phospholipid bilayer integrity. This model emphasises the conformational changes in the protein are coupled to the reorganization of the phospholipid in the membrane bilayer. We further suggest that the BthTx-I homodimer may accumulate a sufficient number of phospholipid molecules to form micelle-like structures that may be released from the protein surface. This proposal is in accord with previous results showing that the BthTx-I promotes the conversion of the liposome membrane bilayer into structures that resemble micelles [19].

In summary, we have demonstrated that at SDS/BthTx-I ratios of between 10 and 40, reversible changes occur in the internal hydrogen bonding of the α-helices, leading to distortions in the conformation of these structures. The structural transitions in the BthTx-I occur at constant SDS/protein ratios over a range of ionic strengths. These events are concomitant with the accumulation of SDS on the surface of the BthTx-I, and the capture of surfactant by the protein raises the total concentration of SDS at which micelles appear in solution. This leads us to conclude that the sequential binding of between 10 and 40 SDS molecules per BthTx-I monomer induces a series of reversible distortions in the α-helices of the protein, and that these changes in protein structure are coupled to a transition in the organization of the associated amphiphiles. Additional study of the association of amphiphiles with the BthTx-I may be useful for a deeper understanding of the coupling between changes protein conformation changes and the organization of bound amphiphiles, which could yield further insights as to the membrane damaging mechanism of the Lys49–PLA_2s.

Acknowledgements

We wish to thank Profs. Drs. João Ruggeiro Neto and Marinônio Lopes Cornélio for access to the spectropolarimeter and the FTIR spectrometer at the Department of Physics-IBILCE-UNESP. The financial support of FAPESP SMOLBnet

project 01/7537-2 (RJW) and doctorate fellowship 97/02749-4 (RKB-B) is gratefully acknowledged. RKB-B is currently the beneficiary of a PRODOC CAPES fellowship. MRB, RKB-B are indebted to Petróleo Brasileiro S.A.-PETROBRAS/Cenpes/ Cognitus Project II.

References

[1] L.L.M. van Deenen, G.H. de Haas, The substrate specificity of phospholipase A_2, Biochim. Biophys. Acta 70 (1963) 538–553.
[2] J. Balsinde, M.V. Winstead, E.A. Dennis, Phospholipase A(2) regulation of arachidonic acid mobilization, FEBS Lett. 531 (2002) 2–6.
[3] C. Yuan, M. Tsai, Pancreatic phospholipase A(2): new views on old issues, Biochim. Biophys. Acta 1441 (1999) 215–222.
[4] O.G. Berg, M.H. Gelb, M.D. Tsai, M.K. Jain, Interfacial enzymology: the secreted phospholipases A_2-paradigm, Chem. Rev. 101 (2001) 2613–2653.
[5] A.R. Peters, N. Dekker, L. van den Berg, R. Boelens, R. Kaptein, A.J. Slotboom, G.H. de Haas, Conformational changes in phospholipase A_2 upon binding to micellar interfaces in the absence and presence of competitive inhibitors. A ^1H and ^{15}N NMR Study, Biochemistry 31 (1992) 10024–10030.
[6] P.M. Kilby, W.U. Primrose, G.C.K. Roberts, Changes in the structure of bovine phospholipase A_2 upon micelle binding, Biochem. J. 305 (1995) 935–944.
[7] B. van den Berg, M. Tessari, R. Boelens, R. Dijkman, G.H. de Haas, R. Kaptein, H.M. Verheij, NMR structures of phospholipase A_2 reveal conformational changes during interfacial activation, Nat. Struct. Biol. 2 (1995) 402–406.
[8] G. Lin, J. Noel, W. Loffredo, H.Z. Stable, M.D. Tsai, Use of short-chain cyclopentano-phosphatidylcholines to probe the mode of activation of phospholipase A_2 from bovine pancreas and bee venom, J. Biol. Chem. 263 (1988) 13208–13214.
[9] D.L. Scott, S.P. White, Z. Otwinowski, W. Yuan, M.H. Gelb, P.B. Sigler, Interfacial catalysis: the mechanism of phospholipase A_2, Science 250 (1990) 1541–1546.
[10] S.A. Tatulian, Toward understanding interfacial activation of secretory phospholipase A_2 (PLA_2): membrane surface properties and membrane-induced structural changes in the enzyme contribute synergistically to PLA_2 activation, Biophys. J. 80 (2001) 789–800.
[11] M.I. Homsi-Brandeburgo, L.S. Queiroz, H. Santo-Neto, L. Rodrigues-Simioni, J.R. Giglio, Fractionation of *Bothrops jararacussu* snake venom: partial chemical characterization and biological activity of bothropstoxin, Toxicon 26 (1988) 615–627.
[12] A.C. Cintra, S. Marangoni, B. Oliveira, J.R. Giglio, Bothropstoxin-I: amino acid sequence and function, J. Protein Chem. 12 (1993) 57–64.
[13] R.J. Ward, L. Chioato, A.H. de Oliveira, R. Ruller, J.M. Sa, Active-site mutagenesis of a Lys49–phospholipase A_2: biological and membrane-disrupting activities in the absence of catalysis, Biochem. J. 362 (2002) 89–96.
[14] J.E. Fletcher, M.S. Jiang, LYS49 phospholipase A_2 myotoxins lyse cell cultures by two distinct mechanisms, Toxicon 36 (1998) 1549–1555.
[15] C. Diaz, J.M. Gutierrez, B. Lomonte, J.A. Gene, The effect of myotoxins isolated from *Bothrops* snake venoms on multilamellar liposomes: relationship to phospholipase A_2, anticoagulant and myotoxic activities, Biochim. Biophys. Acta 1070 (1991) 455–460.
[16] S. Rufini, P. Cesaroni, A. Desideri, R. Farias, F. Gubensek, J.M. Gutierrez, P. Luly, R. Massoud, R. Morero, J.Z. Pedersen, Calcium ion independent membrane leakage induced by phospholipase-like myotoxins, Biochemistry 31 (1992) 12424–12430.
[17] J.Z. Pedersen, B.F. de Arcuri, R.D. Morero, S. Rufini, Phospholipase-like myotoxins induce rapid membrane leakage of non-hydrolyzable ether–lipid liposomes, Biochim. Biophys. Acta 1190 (1994) 177–180.
[18] A.H. de Oliveira, J.R. Giglio, S.H. Andriao-Escarso, A.S. Ito, R.J. Ward, A pH-induced dissociation of the dimeric form of a lysine 49-phospholipase A_2 abolishes Ca^{2+}-independent membrane damaging activity, Biochemistry 40 (2001) 6912–6920.
[19] R.K. Bortoleto-Bugs, A.A. Neto, R.J. Ward, Activation of Ca^{2+}-independent membrane-damaging activity in Lys49–phospholipase A_2 promoted by amphiphilic molecules, Biochem. Biophys. Res. Commun. 322 (2004) 364–372.
[20] P.J. Spencer, S.D. Aird, M. Boni-Mitake, N. Nascimento, J.R. Rogero, A single-step purification of bothropstoxin-1, Braz. J. Med. Biol. Res. 31 (1998) 1125–1127.
[21] F. Szoka Jr., D. Papahadjopoulos, Procedure for preparation of liposomes with large internal aqueous space and high capture by reverse-phase evaporation, Proc. Natl. Acad. Sci. U. S. A. 75 (1978) 4194–4198.
[22] C.A. Marquezin, I.Y. Hirata, L. Juliano, A.S. Ito, Spectroscopic characterization of 2-amino-*N*-hexadecyl-benzamide (AHBA), a new fluorescence probe for membranes, Biophys. Chem. (2006) Article In Press.
[23] M.T. da Silva Giotto, R.C. Garratt, G. Oliva, Y.P. Mascarenhas, J.R. Giglio, A.C. Cintra, W.F. de Azevedo Jr., R.K. Arni, R.J. Ward, Crystallographic and spectroscopic characterization of a molecular hinge: conformational changes in bothropstoxin I, a dimeric Lys49–phospholipase A_2 homologue, Proteins 30 (1998) 442–454.
[24] G.A. Olah, H.W. Huang, Circular dichroism of oriented α-helices. Proof of the exciton theory, J. Chem. Phys. 89 (1988) 2531–2538.
[25] T.M. Cooper, R.W. Woody, The effect of conformation on the CD of interacting helices: a theoretical study of tropomyosin, Biopolymers 30 (1990) 657–676.
[26] M.C. Manning, R.W. Woody, Theoretical CD studies of polypeptide helices: examination of important electronic and geometric factors, Biopolymers 31 (1991) 569–586.
[27] W. Moffitt, The optical rotatory dispersion of simple polypeptides: II, Proc. Natl. Acad. Sci. U. S. A. 42 (1956) 736–746.
[28] G. Holzwarth, P. Doty, The ultraviolet circular dichroism of polypeptides, J. Am. Chem. Soc. 87 (1965) 218–228.
[29] H. Torii, M. Tasumi, in: H.H. Mantsch, D. Chapman (Eds.), Infrared Spectroscopy of Biomolecules, Wiley-Liss Inc, New York, 1996, pp. 1–17.
[30] R.J. Hunter, in: R.J. Hunter (Ed.), Foundations of Colloid Science, Oxford University Press Inc, New York, 2001, p. 435.
[31] S.A. Tatulian, R.L. Biltonen, L.K. Tamm, Structural changes in a secretory phospholipase A_2 induced by membrane binding: a clue to interfacial activation? J. Mol. Biol. 268 (1997) 809–815.
[32] W.A. Pieterson, J.C. Vidal, J.J. Volwerk, G.H. de Haas, Zymogen-catalyzed hydrolysis of monomeric substrates and the presence of a recognition site for lipid–water interfaces in phospholipase A_2, Biochemistry 13 (1974) 1455–1460.
[33] F. Ramirez, M.K. Jain, Phospholipase A_2 at the bilayer interface, Proteins: Structure, Function and Genetics 9 (1991) 229–239.
[34] N.J. Turro, A. Yekta, Luminescent probes for detergent solutions. A simple procedure for determination of the mean aggregation number of micelles, J. Am. Chem. Soc. 100 (1978) 5951–5952.
[35] S.A. Sanchez, Y. Chen, J.D. Muller, E. Gratton, T.L. Hazlett, Solution and interface aggregation states of *Crotalus atrox* venom phospholipase A_2 by two-photon excitation fluorescence correlation spectroscopy, Biochemistry 40 (2001) 6903–6911.
[36] B.Z. Yu, R. Apitz-Castro, M.D. Tsai, M.K. Jain, Interaction of monodisperse anionic amphiphiles with the i-face of secreted phospholipase A_2, Biochemistry 42 (2003) 6293–6301.
[37] O.G. Berg, B.Z. Yu, C. Chang, K.A. Koehler, M.K. Jain, Cooperative binding of monodisperse anionic amphiphiles to the i-face: phospholipase A_2-paradigm for interfacial binding, Biochemistry 43 (2004) 7999–8013.
[38] J.H. van Eijk, H.M. Verheij, R. Dijkman, G.H. de Haas, Interaction of phospholipase A_2 from *Naja melanoleuca* snake venom with monomeric substrate analogs. Activation of the enzyme by protein–protein or lipid–protein interactions? Eur. J. Biochem. 132 (1983) 183–188.
[39] Y.H. Pan, B.Z. Yu, A.G. Singer, F. Ghomashchi, G. Lambeau, M.H. Gelb, M.K. Jain, B.J. Bahnson, Crystal structure of human group X secreted phospholipase A_2. Electrostatically neutral interfacial surface targets zwitterionic membranes, J. Biol. Chem. 277 (2002) 29086–29093.
[40] R.J. Ward, W.F. de Azevedo Jr., R.K. Arni, At the interface: crystal structures of phospholipases A_2, Toxicon 36 (1998) 1623–1633.